



## Synthesis, characterization, and theoretical studies on N'-furan-2ylmethylene-N-[4-(3-methyl-3-phenyl-cyclobutyl)-thiazol-2-yl]-chloro-acetic acid hydrazide

S. Demir, M. Dincer, A. Cukurovali & I. Yilmaz

To cite this article: S. Demir, M. Dincer, A. Cukurovali & I. Yilmaz (2016) Synthesis, characterization, and theoretical studies on N'-furan-2ylmethylene-N-[4-(3-methyl-3-phenyl-cyclobutyl)-thiazol-2-yl]-chloro-acetic acid hydrazide, Molecular Crystals and Liquid Crystals, 629:1, 44-60, DOI: [10.1080/15421406.2015.1106898](https://doi.org/10.1080/15421406.2015.1106898)

To link to this article: <http://dx.doi.org/10.1080/15421406.2015.1106898>



Published online: 16 Jun 2016.



Submit your article to this journal [↗](#)



Article views: 42



View related articles [↗](#)



View Crossmark data [↗](#)

# Synthesis, characterization, and theoretical studies on *N*-furan-2ylmethylene-*N*-[4-(3-methyl-3-phenyl-cyclobutyl)-thiazol-2-yl]-chloro-acetic acid hydrazide

S. Demir<sup>a</sup>, M. Dincer<sup>b</sup>, A. Cukurovali<sup>c</sup>, and I. Yilmaz<sup>c</sup>

<sup>a</sup>Technical Science Vocational High School, Gaziantep University, Gaziantep, Turkey; <sup>b</sup>Department of Physics, Faculty of Arts and Sciences, Ondokuz Mayıs University, Kurupelit, Samsun, Turkey; <sup>c</sup>Department of Chemistry, Faculty of Science, Firat University, Elazığ, Turkey; <sup>d</sup>Department of Chemistry, Faculty of Science, University of Karamanoglu Mehmet Bey, Karaman, Turkey

## ABSTRACT

The title compound, *N*'-furan-2ylmethylene-*N*-[4-(3-methyl-3-phenyl-cyclobutyl)-thiazol-2-yl]-Chloro-acetic acid hydrazide (abbreviated as NNCA), has been synthesized and characterized by elemental analysis, IR, <sup>1</sup>H and <sup>13</sup>C NMR, UV and X-ray single-crystal diffraction. Density function theory (DFT) calculations at the B3LYP/6–31G(d) and 6–31G(d,p) levels for optimized geometries and electronic transition spectra have been performed. In consequence of computing committed for the title compound, the vibrational analysis, molecular electrostatic potential (MEP), frontier molecular orbitals (FMO), theoretical conformational analyses combining molecular mechanics and thermodynamic properties at different temperatures have been obtained.

## KEYWORDS

Crystal structure; Hartree–Fock; thermodynamic properties; vibrational assignment and NMR spectroscopy; density functional method


## 1. Introduction

The molecule which is the subject of this work contains two important functionalities, thiazole and cyclobutane. Thiazole group is what exists in the well-known sulfa drugs and cyclobutane ring in the most popular anticancer drug, carboplatin. [1] On the other hand, cyclobutane itself is of no commercial or biological significance, but more complex derivatives are important in biology and biotechnology. [2] The substances containing these functional groups are very important in medicine as effective compounds with a broad range of activities and in chemistry as starting material in the synthesis of many different chemicals. [1–8] In the light of the knowledge given above, the compounds containing cyclobutane, thiazole, and hydrazone functionalities in one molecule have seen to be important.

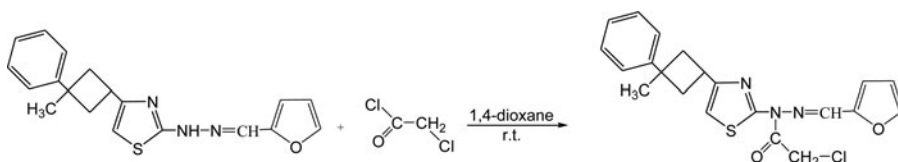
In the present work, we perform FT-IR spectroscopy to make complete vibrational assignments of the infrared spectrum of NNCA molecule in the region 4000–400 cm<sup>–1</sup> through

**CONTACT** S. Demir  [sibeld@gantep.edu.tr](mailto:sibeld@gantep.edu.tr)

Color versions of one or more of the figures in the article can be found online at [www.tandfonline.com/gmcl](http://www.tandfonline.com/gmcl).

 Crystallographic Data (excluding structure factors) have been deposited with the Cambridge Crystallographic Data Centre as supplementary publication Nos. CCDC 775738. Copies of the data can be obtained, free of charge, on application to CCDC, 12 Union Road, Cambridge CB2 1EZ, UK (fax: +44-1223-336033 or e-mail: [deposit@ccdc.cam.ac.uk](mailto:deposit@ccdc.cam.ac.uk)).

© 2016 Taylor & Francis Group, LLC



**Scheme 1.** Reaction sequence of synthesis of the title compound.

density functional theory (DFT) by using B3LYP hybrid functional and Hartree–Fock computation of the vibrational spectrum, NMR spectroscopy, and molecular geometry. In addition to this, HOMO, LUMO, and MEP analyses have been used to elucidate the information regarding charge transfer within the molecule.

The main aim of this paper is to synthesis, characterize, and find theoretical methods that would offer a higher certainty of finding molecular structure parameters and vibrational wavenumbers. As well as a combination of electron correlation effects and basis set deficiencies, the calculated IR spectrum is usually higher than the corresponding experimental frequencies. As known, HF method tends to overestimate vibrational frequencies. In DFT, some correlation effects are taking into account through the effective exchange–correlation potential. Becke’s three parameter exchange functional in combination with the Lee, Yang, and Par (LYP) correlation functional (B3-LYP) and Becke’s exchange functional in combination with the LYP correlation functional (BLYP) were the most widely used for molecular calculations by a fairly large margin. [3,4]

## 2. Experimental and theoretical methods

### 2.1. Experimental

#### 2.1.1. General

The melting point was determined using a capillary tube and a digital melting point apparatus (Gallenkamp Electrothermal) and is uncorrected. Reactions under microwave irradiation were performed in a modified domestic microwave oven (OCEAN OPTICS, HR2000CG). The IR spectrum of the title compound was recorded in the range 3000–400  $\text{cm}^{-1}$  with a MATTSON 1000 FT-IR spectrometer using KBr pellets. The  $^1\text{H}$ -NMR and  $^{13}\text{C}$ -NMR spectra were recorded on a Bruker AVANCE III FT-IR spectrometer (400 MHz) using TMS as an internal standard and chloroform as solvent. All the chemicals and solvents used were of analytical grade.

#### 2.1.2. Synthesis

A solution of 0.3374 gram (1 mmol) of *N*-furan-2-ylmethylene-*N'*-[4-(3-methyl-3-phenyl-cyclobutyl)-thiazol-2-yl]-hydrazine was dissolved in 20 mL of dioxane containing 1 mmol triethylamine. To this solution, 90  $\mu\text{L}$  (1 mmol) of chloroacetyl chloride solution in 20 mL 1,4-dioxane was added dropwise in 2 hr period at room temperature with stirring. Mixture was stirred 2 hr more and then neutralized with 5% aqueous ammonia (if necessary, but generally necessary). The compound thus precipitated was filtered, washed with copious water, and crystallized from ethanol. The reaction path is shown in Scheme 1.

Pale yellow crystals. Yield: 84%. M.p.: 87°C (EtOH). IR (KBr,  $\nu$   $\text{cm}^{-1}$ ): 3121 (–NH–), 2960–2865 (aliphatics), 1709 (C = O), 1619 (C = N thiazole), 737 (>C–Cl), 620 (C–S).  $^1\text{H}$  NMR ( $\text{CDCl}_3$ , TMS,  $\delta$  ppm): 1.58 (s, 3H, –CH<sub>3</sub>), 2.52–2.61 (m, 4H, –CH<sub>2</sub>– in cyclobutane ring), 3.81 (quint,  $j$  = 9.2 Hz, 1H, >CH– in cyclobutane ring), 4.85 (s, 2H, –CH<sub>2</sub>–Cl), 6.48–6.49

**Table 1.** Crystallographic data for title compound.

Formula	C <sub>21</sub> H <sub>20</sub> ClN <sub>3</sub> O <sub>2</sub> S
Formula weight	413.91
Temperature (K)	296
Wavelength (Å)	0.71073
Crystal system	Orthorhombic
Space group	P 2 <sub>1</sub> 2 <sub>1</sub> 2 <sub>1</sub>
<i>a</i> (Å)	5.8951 (10)
<i>b</i> (Å)	17.3663 (9)
<i>c</i> (Å)	20.253
$\alpha$ (°)	90
$\beta$ (°)	90
$\gamma$ (°)	90
<i>V</i> (Å <sup>3</sup> )	2073.4 (4)
<i>Z</i>	4
<i>D</i> <sub>calc</sub> (g/cm <sup>3</sup> )	1.326
<i>F</i> (000)	864
<i>hkl</i> Range	−6 ≤ <i>h</i> ≤ 7 −20 ≤ <i>k</i> ≤ 20 −24 ≤ <i>l</i> ≤ 19
Reflections collected	11513
Independent reflections	2114
<i>R</i> <sub>int</sub>	0.040
Reflections observed [ <i>I</i> ≥ 2σ( <i>I</i> )]	1489
<i>R</i> [ <i>I</i> > 2σ( <i>I</i> )]	0.031
<i>Rw</i> [ <i>I</i> > 2σ( <i>I</i> )]	0.068
Goodness-of-fit on indicator	0.82
Structure determination	Shelxs-14
Refinement	Full matrix
(Δσ) <sub>max</sub> , (Δσ) <sub>min</sub> (e/Å <sup>3</sup> )	0.09, −0.12

(dd,  $j_1 = 3.7$  Hz,  $j_2 = 1.8$  Hz 1H, in furan), 6.56 (d,  $j = 3.66$  Hz, 1H, in furan ring), 6.88 (s, 1H, = CH-S in thiazole ring), 7.16–7.21 (m, 3H, aromatics), 7.26–7.32 (m, 2H, aromatics), 7.54 (d,  $j = 1.5$  Hz, 1H, aromatics), 8.93 (s, 1H, -N = CH-). <sup>13</sup>C NMR (CDCl<sub>3</sub>, TMS, δ ppm): 167.77, 156.91, 152.38, 149.15, 145.53, 140.28, 128.49, 125.59, 124.93, 115.61, 112.30, 112.06, 43.96, 41.18, 39.01, 30.97, 30.23. Anal. calc. for C<sub>21</sub>H<sub>20</sub>ClN<sub>3</sub>O<sub>2</sub>S (413.92); C: 60.94, H: 4.87, N: 10.15, S: 7.75; found; C: 60.71, H: 5.00, N: 10.34, S: 7.55.

### 2.1.3. Crystallography

The diffraction data of the title compound were collected at  $T = 296$  K on an STOE diffractometer with an IPDS(II) image plate detector equipped with a graphite-monochromatic Mo- $K\alpha$  radiation ( $\lambda = 0.71073$  Å) using an  $\omega$  scan mode in the range of  $1.5 \leq \theta \leq 25^\circ$ . The structure was solved by direct methods and refined by full-matrix least-squares on  $F^2$  with SHELXL [5] software package. All non-hydrogen atoms were anisotropically refined. The hydrogen atoms were fixed geometrically at the calculated positions and allowed to ride on the parent carbon atoms. The final  $R = 0.031$  and  $Rw = 0.068$  ( $w = 1/[\sigma^2(F_o^2) + (0.0812P)^2]$ , where  $P = (F_o^2 + 2F_c^2)/3$ ) for 1489 observed reflections with  $I > 2\sigma(I)$ . The molecular graphics was plotted using SHELXTL. Atomic scattering factors and anomalous dispersion corrections were taken from International Tables for X-ray crystallography. [6] A summary of the key crystallographic information is given in Table 1.

### 2.2. Theoretical

The geometry optimizations of the molecules in gas phase were carried out without any symmetry restrictions. Ground state structure has been confirmed by frequency analyses. In order

**Table 2.** Hydrogen bonding geometry (Å, °) for the title compound.

D—H...A (Å)	D—H (Å)	H...A (Å)	D...A (Å)	D—H...A(deg)
C7—H7b ...N1	0.97	2.76	3.076	149
C15—H15 ...N1	0.93	2.10	2.754(3)	126
C4—H4 ...Cg(3)	0.98	2.81	3.784(2)	174
C11—H11 ...Cg(4)	0.93	2.91	3.623(3)	134

Cg(3):O1-C16, Cg(4): C9-C14.

to calculate the  $\lambda_{\max}$  values in the UV-vis spectra, corresponding to the vertical excitation energies and oscillator strengths, the DFT method [7,8] was used with functionals and basis sets in geometry optimizations. Electronic absorption spectra were calculated by DFT method at the B3LYP/6-31G\* level. In order to obtain the most stable ground-state geometries, the two different basis sets, 6-31G(d), 6-31G(d,p) with B3LYP [9,10] and HF functionals and were used.

The geometry of the title compound, together with that of tetramethylsilane (TMS), is fully optimized.  $^1\text{H}$ - and  $^{13}\text{C}$ -NMR chemical shifts were calculated within the GIAO approach [11,12] applying the same methods and basis sets as used for geometry optimization. The  $^1\text{H}$  and  $^{13}\text{C}$ -NMR chemical shifts were converted to the TMS scale by subtracting the calculated absolute chemical shielding of TMS ( $\delta = \Sigma_0 - \Sigma$ , where  $\delta$  is the chemical shift,  $\Sigma$  is the absolute shielding and  $\Sigma_0$  is the absolute shielding of TMS), with values of 32.52 and 199.79 ppm for HF/6-31G(d) and 32.10 and 189.40 ppm for B3LYP/6-31G(d), respectively. Vibrational frequencies calculated ascertain the structure is stable as no imaginary frequencies were observed. The thermodynamic properties of the title compound at different temperatures were calculated on the basis of vibrational analyses.

All calculations were performed using the GaussView Molecular Visualization program [13] and Gaussian 03 program package [14] on a personal computer without specifying any symmetry for the title molecule. The effect of solvent on the theoretical NMR parameters was included using the default model IEF-PCM (Integral-Equation-Formalism Polarizable Continuum Model) [15] provided by Gaussian 03. Chloroform ( $\text{CDCl}_3$ ), with a dielectric constant ( $\epsilon$ ) of 4.90 was used as solvent.

### 3. Results and discussion

#### 3.1. Description of the crystal structure

The displacement ellipsoid plot with numbering scheme for the title compound is shown in Fig. 1. Fig. 2 depicts a perspective view of the crystal packing in the unit cell. The selected bond lengths, bond angles, and torsion angles by X-ray diffraction are listed in Table 2 along with the calculated bond parameters.

The asymmetric unit in the crystal structure contains only one molecule. The molecular structure of  $\text{C}_{21}\text{H}_{20}\text{ClN}_3\text{O}_2\text{S}$ , NNCA, consists of a central thiazole ring which is fused to a cyclobutyl ring with chloro acetic acid hydrazide bonded at the C1 and C2 positions, respectively, around this fused-ring moiety. The C-S bond lengths of thiazole ring of 1.701(4) and 1.726(2) Å is longer than 1.694(2) and 1.719(2) Å for a similar structure.[16] Literature value for the puckering of the cyclobutane ring are 23.8(3)°, [17] and 25.74(6)°. [18] The geometry of the cyclobutane ring is influenced by the steric effect of the different groups. However, when the bond lengths and angles of the cyclobutane ring in the title compound are compared with these, it is seen that there are no significant differences. In this paper, the C5/C6/C7 plane

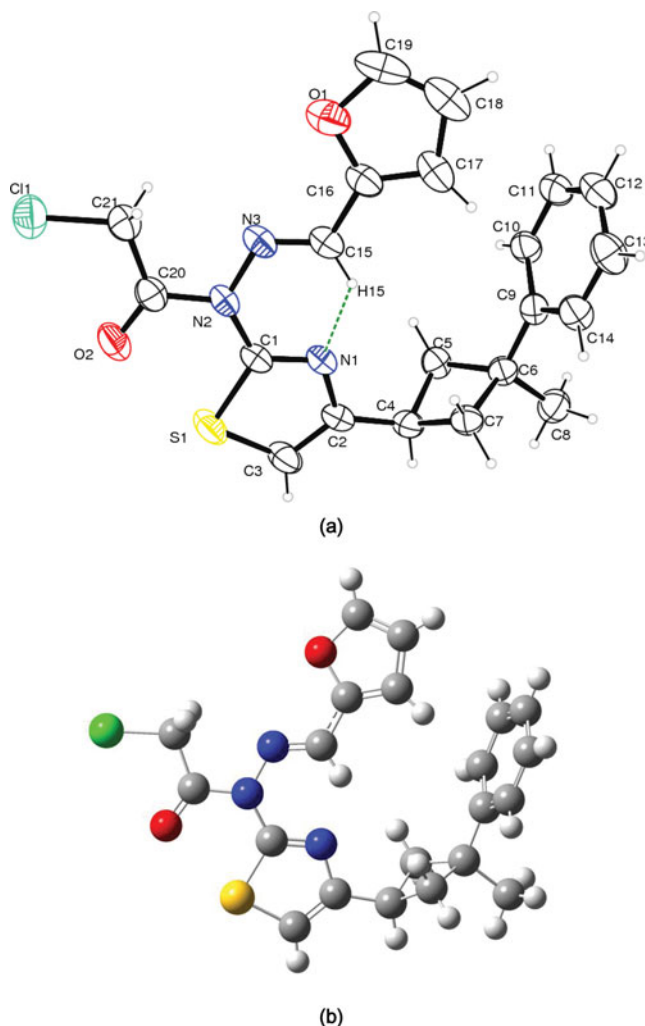


**Figure 1.** (a) ORTEP diagram of Wingx. The thermal ellipsoids are drawn at the 40% probability level. (b) DFT optimized structure of NNCA of GaussView.

forms a dihedral angle of  $20.34(23)^\circ$  with the C5/C4/C7 plane. This value is smaller than those in the literatures.

Strong intramolecular C–H...N hydrogen bond interactions (Table 2) exist with C7–H7b...N1 forming a pseudo-five-membered ring of N(5) graph-set motif. [19] Weak C–H...N intramolecular contacts with C15–H15...N1 forming a second pseudo-six-membered ring of N(6) graph-set motif [19] also influence crystal packing. [20] There are no hydrogen bond,  $\pi$ – $\pi$  stacking interactions present in the structure of NNCA, which is in contrast to the presence of such interactions in similar structures reported earlier. [21–24] It is noted that these structures all crystallize in the monoclinic or triclinic space group while the title compound here crystallizes in the orthorhombic space group. [25]

### 3.2. Vibrational spectra

Experimentally, the FT-IR spectrum of the title compound is shown in Fig. 3. By using GaussView, [26] molecular visualization program, the vibrational bands assignments have

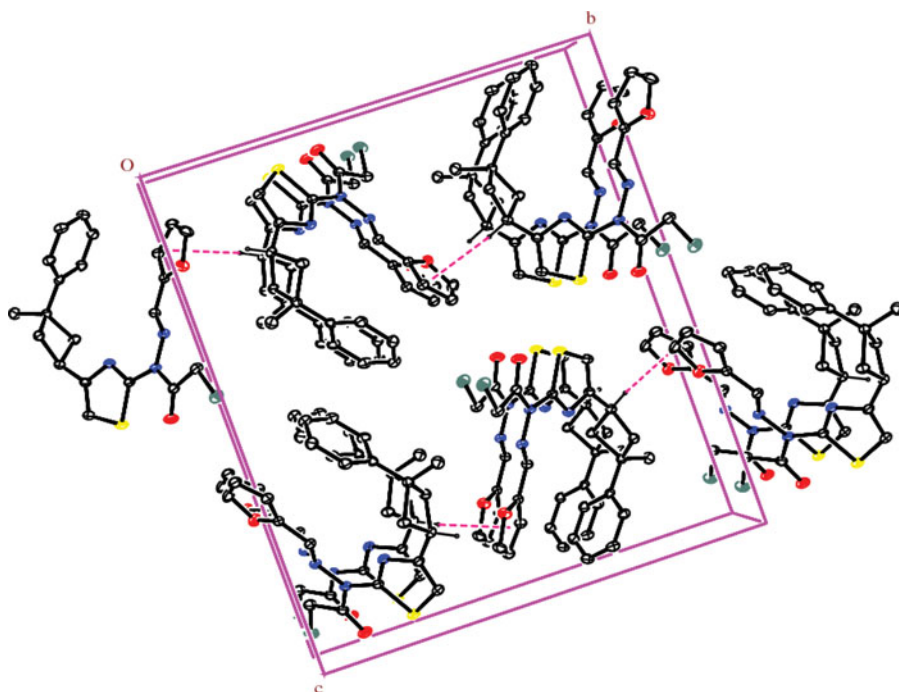


**Figure 2.** Packing diagram of the title compound.

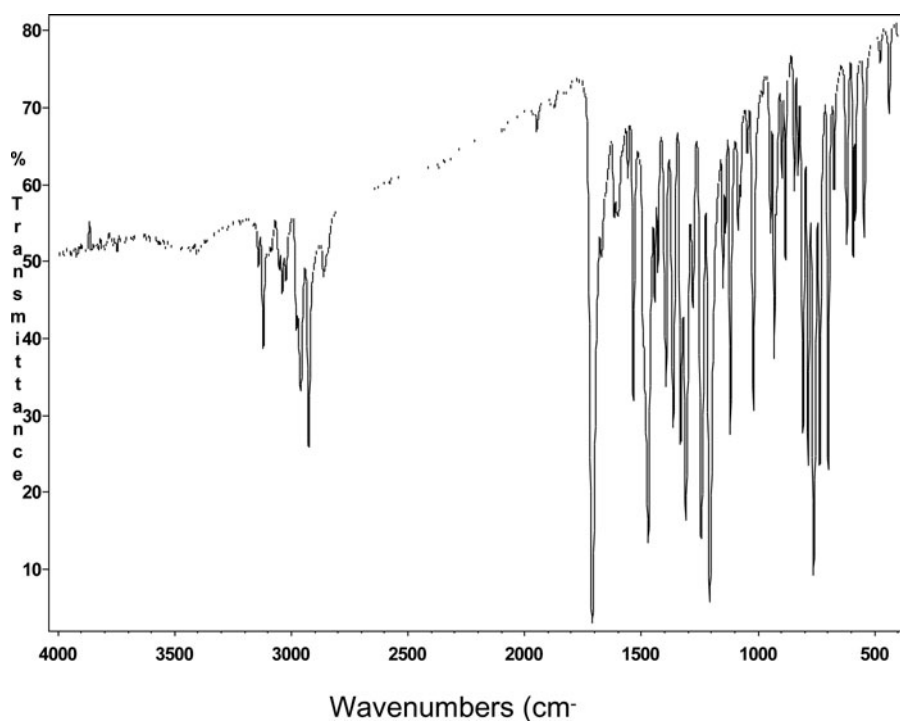


**Figure 3.** FT-IR spectrum of the title compound.



been made. In order to investigate that intermolecular hydrogen bond influences on the vibrational frequencies, we have calculated the theoretical harmonic vibrational spectra of the title compound by using B3LYP and HF methods with 6-31G(d) and 6-31G(d,p) basis sets. To facilitate assignment of the observed peaks, we have analyzed vibrational frequencies and compared our calculation of the title compound with their experimental results and shown in Table 3. Consequently, the Hartree-Fock calculated results are usually more overestimated than the corresponding DFT values. [27]

The bands calculated in the measured region 4000–400  $\text{cm}^{-1}$  arise from the vibrations of C-H, C = O, C = N, N-N stretching, and the internal vibrations, etc. of the title compound. For the assignments of  $\text{CH}_2$  group frequencies (in chloro acetic acid), four fundamental vibrations can be associated to  $\text{CH}_2$  groups. One asymmetric stretching, one stretching, one scissoring, and one wagging vibration mode designated the motion of the methylene group. The  $\text{CH}_2$  stretching vibration is established at 3080  $\text{cm}^{-1}$  and the  $\text{CH}_2$  asymmetric stretching vibration is established at 3120  $\text{cm}^{-1}$  in the spectra. In the present study various vibrations of  $\text{CH}_2$  group are summarized in Table 3. In the spectra, the  $\text{CH}_3$  asymmetric stretching vibration is established at 3268/3262 and 3246  $\text{cm}^{-1}$ , whereas  $\text{CH}_3$  symmetric stretching vibration is established at 3198 and 3177  $\text{cm}^{-1}$ , for HF/6-31G(d) and 6-31G(d,p) method, the  $\text{CH}_3$  asymmetric and symmetric stretching vibrations are calculated at 3107–3039  $\text{cm}^{-1}$  and 3107–3035  $\text{cm}^{-1}$  for B3LYP/6-31G(d) and 6-31G(d,p) method, respectively.

In the thiazole, C-C and C-S stretching modes were observed to be 1599 and 620  $\text{cm}^{-1}$  as experimentally, 1778 and 925/803  $\text{cm}^{-1}$  for HF/6-31G(d) level, 1777 and 924  $\text{cm}^{-1}$  for HF/6-31G(d,p) level, 1587 and 853/737/624  $\text{cm}^{-1}$  for B3LYP/6-31G(d) level, 1586 and 852  $\text{cm}^{-1}$  for B3LYP/6-31G(d,p) level.

Other essential characteristic vibrations of the title compound are C = O and C-Cl stretching modes were observed to be 1619 and 737  $\text{cm}^{-1}$  as experimentally. These modes were calculated at 2008 and 885  $\text{cm}^{-1}$  for HF/6-31G(d), 2007 and 884  $\text{cm}^{-1}$  for HF/6-31G(d,p) level, 1799 and 813  $\text{cm}^{-1}$  for B3LYP 6-31G(d) level, 1799 and 812  $\text{cm}^{-1}$  for B3LYP/6-31G(d,p) level. Also, the other levels of calculations can be seen in Table 3.

### 3.3. NMR spectra

The recent development of methods for quantum mechanical calculations of NMR parameters has guided the study of a wide range of chemical problems. [28,29] These have regarded mainly the most common NMR-active nuclei usually considered in structural chemistry, such as  $^{31}\text{P}$ ,  $^{15}\text{N}$ ,  $^1\text{H}$ ,  $^{17}\text{O}$ , and  $^{13}\text{C}$ , and more recently this approach has investigated a number of less conventional nuclei. GIAO chemical shift calculation, [30] for organic molecules has recently emerged as one of the most promising new approaches in structure elucidation. In this regard, we have recently shown that the GIAO calculations of  $^{13}\text{C}$  c.s. can be very helpful in the validation of low polarity rigid molecular structures, [31] and for the determination of the relative configuration of flexible compounds. [32] Also, it has been shown that spin-spin coupling constant calculations at DFT level may be very useful for the comprehension of the multiplicity of the  $^1\text{H}$  spectra of organic compounds and as a support in the interpretation of the NMR parameters necessary for extensive conformational analysis. [33–35] Moreover, we have recently compared different theory models and basis sets in the calculation of  $^{13}\text{C}$  NMR chemical shifts of natural products in order to suggest a convenient and consistent protocol to be employed for the reproduction of the experimental  $^{13}\text{C}$  spectra of organic molecules, by using different combinations of geometry optimization methods and single point  $^{13}\text{C}$  chemical shift calculations, both using different theory levels and different basis sets.[36]





**Table 3.** Comparison of the observed and calculated vibrational spectra of the title compound.

Assignments	Experimental IR ile KBr (cm <sup>-1</sup> )	HF 6-31G(d)	6-31G(d,p)	Calculated B3LYP 6-31G(d)	6-31G(d,p)
$\nu_{\text{str}}$ (CH) hydrazide	3405	3462	3437	3221	3208
$\nu_{\text{str}}$ (CH) thiazole	3214	3443	3426	3267	3263
$\nu_{\text{sym-str}}$ (CH) phenyl	3141	3385	3369	3207	3204
$\nu_{\text{asym-str}}$ (CH2) chl. act. acid	3120	3384	3362	3187	3181
$\nu_{\text{asym-str}}$ (CH) phenyl	3051	3374/3365/3350	3350–3333	3180/3176	3186/3177/3173
$\nu_{\text{str}}$ (CH2) chl. act. acid	3038	3322	3300	3134	3126
$\nu_{\text{asym-str}}$ (CH2) + $\nu_{\text{str}}$ (CH) cyclobutane	3023	3295/3291	3280	3133/3129	3131
$\nu_{\text{asym-str}}$ (CH3)	2979	3268/3262	3246	3107	3107
$\nu_{\text{sym-str}}$ (CH2) + $\nu_{\text{str}}$ (CH) cyclobutane	2959	3250/3233	3235–3212	3084/3071	3067
$\nu_{\text{sym-str}}$ (CH2) cyclobutane	2926	3230	3276	3067	3063
$\nu_{\text{sym-str}}$ (CH3)	2856	3198	3177	3039	3035
$\nu_{\text{str}}$ (C = O)	1709	2008	2007	1799	1799
$\nu_{\text{str}}$ (C = N) hydrazide	1827	1914	1913	1677/	1675
$\nu_{\text{str}}$ (C-C) phenyl	1711	1809/1778	1807/1776	1662/1637	1659/1634
$\nu_{\text{str}}$ (C-C)furan	1670	1792	1791	1619	1618
$\nu_{\text{str}}$ (C-C) thiazole	1599	1778	1777	1587	1586
$\nu_{\text{str}}$ (C = N) + $\nu_{\text{str}}$ (C-C) + $\nu_{\text{rock}}$ (CH) thiazole	1558	1700	1699	1538	1537
$\nu_{\text{str}}$ (C-C) furan + $\nu_{\text{str}}$ (C = N) thiazole	1619	1676	1675	1524	1523
$\nu_{\text{rock}}$ (CH) phenyl	1534	1671/1610/1475	1665/1604	1491	1486/1485
$\nu_{\text{str}}$ (C-N) + $\nu_{\text{rock}}$ (CH)hydrazide	1394	1537/1210	1533	1405	1401
$\nu_{\text{rock}}$ (CH) cyclobutane + $\nu_{\text{rock}}$ (CH)thiazole	1363	1511	1501	1382	1373
$\nu_{\text{wag}}$ (CH2) chl. act. acid	1332	1490	1482	1342	1335

(Continued)

Table 3. (Continued)

Assignments	Experimental IR ile KBr (cm <sup>-1</sup> )	HF 6–31G(d)	6–31G(d,p)	Calculated B3LYP 6–31G(d)	6–31G(d,p)
$\nu_{\text{str}}$ (C-N)thiazole+ $\nu_{\text{wag}}$ (CH2) chl. act. acid	1309	1477	1473	1352	1269
$\nu_{\text{wag}}$ (CH2)+ $\nu_{\text{str}}$ (C-C) cyclobutane	1279	1459	1453	1333	1248
$\nu_{\text{str}}$ (C-N-N)	1244	1420	1419	1273	1228
$\nu_{\text{str}}$ (C-O) furan+ $\nu_{\text{wag}}$ (CH2) chl. act. acid+ $\nu_{\text{rock}}$ (CH)furan	1206	1415	1412	1273	1194
$\nu_{\text{str}}$ (C-N)+ $\nu_{\text{wag}}$ (CH2)+ $\nu_{\text{rock}}$ (CH)hydrazide	1197	1365	1360	1251/1232	1247
$\nu_{\text{twist}}$ (CH2) cyclobutane	1150	1216/1165	1288/1161	1189/1075	1070
$\nu_{\text{str}}$ (N-N)	1138	1180	1180	1065	1064
$\nu_{\text{out of plane}}$ (CH)hydrazide	1118	1133	1133	1004	1006
$\nu_{\text{str}}$ (C-C) chl. act. acid+ $\nu_{\text{str}}$ (C-N)thiazole	1085	1129	1127	1045	936
$\nu_{\text{twist}}$ (CH) phenyl	1075	1123/1103/1102/1037	1122/1103/1036	992/968/926/861	996
$\nu_{\text{scr}}$ (CH)furan	1045	1110	1107	1052	1049
$\nu_{\text{breath}}$ phenyl	1019	1088	1087	1065/1077/634	1054/1015
$\nu_{\text{breath}}$ cyclobutane	981	1047	1044	1008	1043
$\nu_{\text{breath}}$ furan	947	1042/863	1041	1120/954/900	1118/954
$\nu_{\text{breath}}$ thiazole	930	981/678	980	1045/911	899
$\nu_{\text{bending}}$ furan	923	972	972	683	683
$\nu_{\text{str}}$ (C-S)	620	925/803	924	853/737/624	852
$\nu_{\text{str}}$ (C-Cl)	737	885	884	813	812
$\nu_{\text{out of plane}}$ (CH)thiazole	781	869	868	754	754
$\nu_{\text{wag}}$ furan	761	868	868	760	762
$\nu_{\text{wag}}$ phenyl	735	859	859	782	781
$\nu_{\text{out of plane}}$ thiazole	699	774	773	703/606	754
$\nu_{\text{bending}}$ (C-N-N)	673	687	686	633	633/624
$\nu_{\text{bending}}$ (C = N-N)	477	475	475	440	440

**Table 4.** Theoretical and experimental  $^{13}\text{C}$  and  $^1\text{H}$  isotropic chemical shifts (with respect to TMS all values in ppm) for the title compound.

Atom	Experimental ( $\text{CDCl}_3$ )	Calculated chemical shift (ppm)			
		HF 6–31G(d)	6–31G(d,p)	B3LYP 6–31G(d)	6–31G(d,p)
C1	167.54	163.27	167.55	148.12	152.77
C2	155.04	145.21	145.53	146.17	150.92
C3	111.82	105.22	108.74	98.06	101.47
C4	30.74	25.64	29.02	16.48	19.74
C5	43.68	33.99	37.14	22.9	25.47
C6	38.78	31.83	35.68	30.22	34.46
C7	43.68	33.99	37.15	23.91	26.5
C8	29.97	27.85	30.85	7.31	9.41
C9	148.93	148.98	153.7	143.51	148.54
C10	124.70	121.68	125.36	108.59	112.04
C11	128.25	125.23	129.12	111.83	115.4
C12	125.35	121.18	125	107.27	110.81
C13	128.25	125.23	129.13	111.4	114.98
C14	115.34	121.67	125.35	109.92	113.35
C15	140.07	137.23	140.86	128.1	131.64
C16	152.14	139.32	143.96	135	140
C17	115.34	115.03	118.58	104.35	107.83
C18	112.52	104.56	108.45	97.52	101.29
C19	145.28	139.16	142.77	133.87	137.42
C20	156.69	164.78	168.95	157.2	161.6
C21	40.96	43.17	46.68	36.54	39.66
H3	6.88	6.1	7.06	2.87	3.95
H4	3.81	3.1	3.81	0.29	0.97
H5*	2.52	2.22	2.92	0.95	0.29
H7*	2.61	2.22	2.92	0.88	0.23
H8*	1.58	9.04	1.79	3.20	2.60
H10	7.16	7.25	8.07	4.45	5.39
H11	7.54	7.48	8.29	4.69	5.62
H12	7.21	7.36	8.17	4.62	5.55
H13	7.32	7.48	8.29	4.86	5.8
H14	7.26	7.25	8.07	4.65	5.6
H15	8.93	9.59	10.5	6.7	7.85
H17	6.48	5.21	6.13	1.79	2.82
H18	6.49	6	6.96	3.12	4.18
H19	6.56	7.4	8.23	4.65	5.71
H21*	4.85	4.19	4.99	1.34	2.08

\*: Average.

GIAO  $^{13}\text{C}$  and  $^1\text{H}$  chemical shift calculations have been carried out using the HF and B3LYP methods with 6–31G(d) and 6–31G(d,p) basis sets for the optimized geometry. The results of these calculations are tabulated in Table 4. DFT methods treat the electronic energy as a function of the electron density of all electrons simultaneously and thus include electron correlation effect. The experimental and calculated  $^1\text{H}$  NMR and  $^{13}\text{C}$  NMR chemical shifts are compared in Table 4 (the atom numbering is in line with Fig. 1).

Since experimental  $^1\text{H}$  chemical shift values were not available for individual hydrogen, we have presented the average values for  $\text{CH}_2$  and  $\text{CH}_3$  hydrogen atoms. We have calculated  $^1\text{H}$  chemical shift values (with respect to TMS) of 9.04–2.22 ppm and 8.29–1.79 ppm (HF/6–31G(d) and HF/6–31G(d,p)), and 6.7–0.29 ppm and 7.85–0.23 ppm (B3LYP/6–31G(d) and B3LYP/6–31G(d,p)); however, the experimental results were observed to be 8.93–1.58 ppm, these values are shown in Table 4 and so the accuracy ensures reliable interpretation of spectroscopic parameters. Also, the difference is related to bond lengths in the between hydrogen and other atoms. The  $-\text{CH}_2-$  signals of the cyclobutane are observed at 2.52 and 2.61 ppm. The C-H signals belonging to furan ring are shielded at 6.48, 6.49, and 6.56 ppm. However,

the C-H signals of phenyl adjacent to the cyclobutane are deshielded at 7.16–7.54 ppm. The singlet signal of the methyl group is observed at 1.58 ppm.

The experimental  $^{13}\text{C}$  spectra data also support the structure of the compound.  $^{13}\text{C}$ -NMR spectra of the thiazole compound show the signals at 156.91 and 149.15 ppm due to C atoms next to sulfur atom. These signals have been calculated as 163.27–105.22 ppm and 167.55–108.74 ppm for HF levels, 148.12–98.06 ppm and 152.77–101.47 ppm for B3LYP levels. While the C atoms of methylene group belonging to the cyclobutane ring are observed at 41.18 and 39.01 ppm, methine C atom appeared at 30.23 ppm. The signal at 30.97 ppm is related to the last C atom of the cyclobutane ring.

As already observed for the  $^{13}\text{C}$  c.s., also for the GIAO  $^1\text{H}$  calculations, HF methods show a very good agreement with the experimental results, and they usually perform better than the DFT methods (Table 4).

### 3.4. Theoretical structures

In DFT calculation, hybrid functionals are also used, the Becke's three-parameter functional (B3), [37] which defines the exchange functional as the linear combination of Hartree-Fock, local and gradient-corrected exchange terms. The B3 hybrid functional was used in combination with the correlation functionals of Lee, Yang, and Parr. [38] The optimized parameters (bond lengths, bond angles, and dihedral angles) of the title compound were obtained using the B3LYP/6–31G(d) and 6–31G(d,p) method. The results are listed in Table 5 and compared with the experimental data for the title compound. It is well known that DFT-optimized bond lengths are usually longer and more accurate than HF, due to the inclusion of electron correlation. But, according to our calculations, the HF method correlates well for the bond length compared with the other method (Table 5). Although the largest difference between experimental and calculated bond lengths is about 0.051 Å for HF and 0.043 Å for B3LYP, the root mean square error (RMSE) is found to be about 0.068 Å for HF and 0.21 Å for B3LYP, indicating that the bond lengths obtained by the HF method show the strongest correlation with the experimental values. The same trend was also observed for bond angles. However, this time, both the largest difference and the RMSE for the bond angles obtained by the HF (6–31G(d) basis set) method are smaller than those determined by B3LYP.

A global comparison was performed by superimposing the molecular skeletons obtained from X-ray diffraction and the theoretical calculations atom by atom (Fig. 4), obtaining RMSE values of 0.373, 0.368, and 0.396, 0.394 Å for A (for B3LYP) and B (for HF), respectively. According to this result, the smallest RMSE value is obtained for molecule A and the geometry obtained from this molecule coincides better with the crystalline structure than molecule B.

### 3.5. Conformational analysis

The energy based conformational searching techniques, concerning the level of calculation utilized to establish conformation and following this to evaluate energies and other properties as a function of conformation, is a considerable computational request and is still an active area of research. One of the reasonable alternatives, when the property of interest is energy, is the following: full conformational search using molecular mechanics followed by geometry optimization using semiempirical model for selected conformers and finally single-point calculation using ab initio models for selected conformers. [39] Starting molecules were built from structural fragments using standard geometry. Before conformation search, we obtained stable molecules by performing geometry optimization with the semiempirical AM1, [40]

**Table 5.** Selected optimized and experimental geometries parameters of the title compound in ground state.

Parameters	Experimental	Calculated			
		HF 6–31G(d)	6–31G(d,p)	DFT/B3LYP 6–31G(d)	6–31G(d,p)
<b>Bond lengths (Å)</b>					
N2–N3	1.400(3)	1.371	1.371	1.383	1.383
C15–N3	1.266(3)	1.258	1.258	1.289	1.290
N2–C1	1.412(3)	1.400	1.400	1.410	1.409
C2–N1	1.385(3)	1.382	1.382	1.383	1.383
C3–S1	1.701(3)	1.731	1.730	1.739	1.739
C1–S1	1.726(2)	1.747	1.746	1.769	1.769
C20–O2	1.201(3)	1.186	1.186	1.214	1.214
C21–C11	1.765(3)	1.774	1.774	1.795	1.795
C4–C5	1.548(3)	1.547	1.547	1.558	1.558
C5–C6	1.545(4)	1.553	1.553	1.563	1.563
C6–C7	1.555(3)	1.553	1.553	1.563	1.563
C4–C7	1.536(4)	1.547	1.547	1.558	1.558
C2–C3	1.348(4)	1.337	1.337	1.363	1.363
O1–C19	1.390(4)	1.339	1.339	1.357	1.357
O1–C16	1.346(4)	1.346	1.346	1.371	1.370
RMSE <sup>a</sup>		0.068	0.068	0.21	0.21
Max. difference <sup>a</sup>		0.051	0.051	0.043	0.043
<b>Bond angles (°)</b>					
C11–C21–C20	111.0(2)	111.383	111.410	111.080	111.139
O2–C20–C21	124.6(3)	123.572	123.586	124.025	124.048
O2–C20–N2	121.0(3)	121.383	121.355	121.297	121.279
C1–N2–N3	125.6(2)	126.321	126.306	127.116	127.081
C1–N1–C2	111.4(2)	112.156	112.152	111.884	111.877
C1–S1–C3	87.94(14)	87.945	89.470	87.710	87.729
C4–C5–C6	89.7(2)	89.502	89.494	89.678	89.679
C4–C6–C7	89.8(2)	89.502	89.494	89.677	89.679
RMSE <sup>a</sup>		0.566	0.780	0.61	0.64
Max. difference <sup>a</sup>		1.028	1.53	1.516	1.481
<b>Torsiyon angles (°)</b>					
N1–C1–N2–N3	–3.9(4)	0.029	0.025	0.038	–0.008
C1–N2–C20–O2	9.3(4)	0.003	–0.002	–0.014	0.001
C11–C21–C20–O2	–4.8(4)	0.007	–0.048	0.011	–0.004
N2–C1–N1–C2	–176.8(2)	–179.996	–179.991	–179.994	179.997
N3–N2–C1–S1	178.2(2)	–179.969	–179.970	–179.957	179.990

<sup>a</sup> RMSE and maximum differences between the bond lengths and angles computed by the theoretical methods and those obtained from X-ray diffraction.

method. In the case of conformational analyses NNCA, we chose a 10° grid step for all single bonds between nonterminal, non-hydrogen atoms. The particular role played by the  $\varphi$  torsional angle in the characterization of the backbone structure of NNCA deserves a detailed study, namely by mapping the potential energy profile around these coordinate. [41] Taking NNCA as the starting structure, successive rotations about  $\varphi$  using a 10° scanning step were performed. The resulting potential energy profile is depicted in Fig. 5. Firstly, the minimum energy occurs at  $\varphi = 120^\circ$ . Two other minima at  $\varphi = 100^\circ$  and  $\varphi = 110^\circ$  with energies of ca. 0.15037 a.u. above the first were also observed.

As it was already mentioned above, we are not aware of any experimental or theoretical study performed on NNCA in the gas phase to be compared with our results. Consequently, most stable conformer predicted by our AM1 theoretical calculations.

### 3.6. Molecular electrostatic potential

Molecular recognition and the converse concept of specificity, [42] are explained in mechanistic and reductionistic terms by a stereoelectronic complementarity between the binding molecule and the receptor. [43] The intermolecular forces that contribute to both affinity and

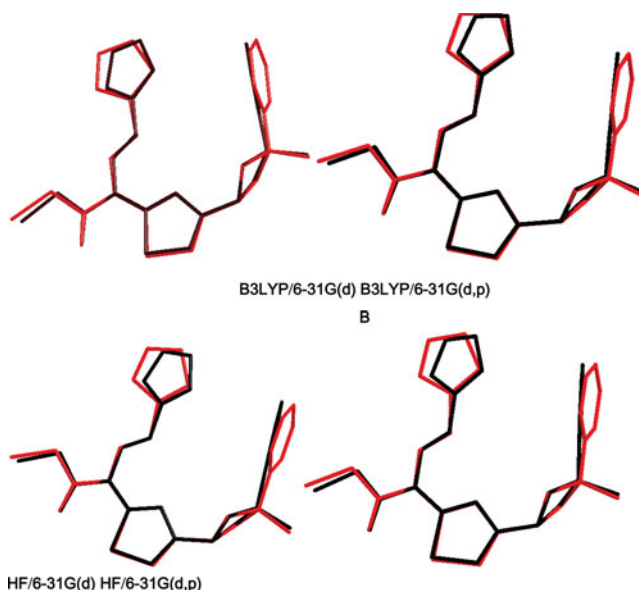


**Figure 4.** Atom-by-atom superimposition of the structures calculated (red) [A = B3LYP, B = HF] over the X-ray structure (black) for the title compound. Hydrogen atoms omitted for clarity.

specificity can be schematically classified as hydrophobic and electrostatic ones. Thus, MEPs are of particular value because they permit visualization and assessment of the capacity of a molecule to interact electrostatically with a binding site. MEPs can be interpreted in terms of a stereoelectronic pharmacophore condensing all available information on the electrostatic forces underlying affinity and specificity.

To predict reactive sites for electrophilic attack for NNCA, MEP was calculated at the B3LYP/6-31G(d) optimized geometry. The negative (red) regions of MEP were related to electrophilic reactivity and the positive (blue) ones to nucleophilic reactivity shown in Fig. 6. The MEPs exhibit three clear minimum values (deep red zones) in the vicinity of Chloroacetic acid group and furan ring.

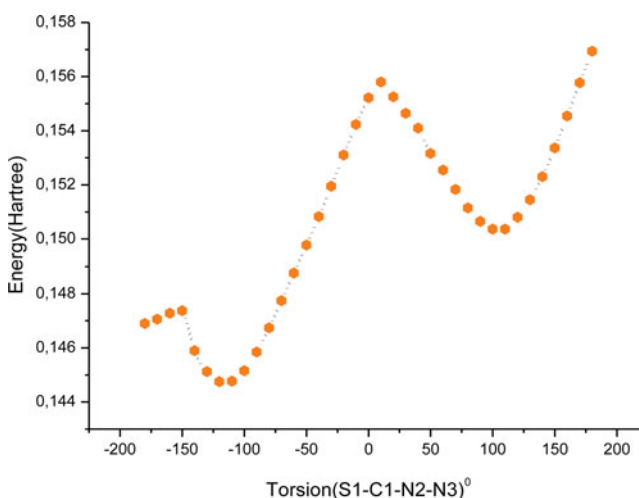


**Figure 5.** Molecular energy profile of the optimized counterpart of the title compound versus selected degrees of torsional freedom.

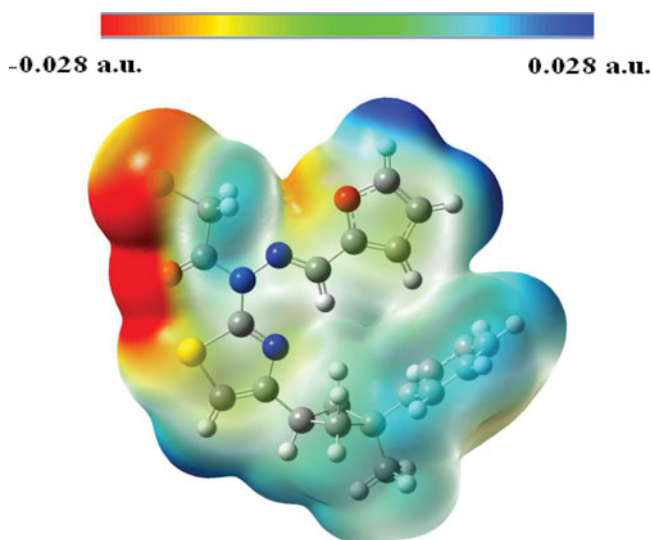


**Figure 6.** Molecular electrostatic potential map calculated at B3LYP/6–31G(d) level.

### 3.7. Electronic absorption spectra

Based on the optimized geometry at the B3LYP/6–31G\* level, electronic absorption spectra were calculated by using DFT method at the B3LYP/6–31G\* level. The calculations indicate that the compound has 112 occupied molecular orbitals (MOs). An electronic system with a larger HOMO–LUMO gap should be less reactive than one having a smaller gap. [44] The HOMO–LUMO gap value of the molecule is [If the electron correlations had not been included, the energy difference HOMO–LUMO would be nearly 10 eV], 4.237 eV for B3LYP/6–31G\* level.

The compound exhibits absorption peaks in the UV-visible region. All experiments and theoretical calculations acquire two absorption bands. The absorption peaks are observed at 281.9 and 249.2 nm for the title compound. It can be seen that these peaks equal to  $n-\pi^*$  and  $\pi-\pi^*$  transitions. Additionally, in the experiments, the wavelength belonging to the HOMO–LUMO transition, and thus the maximum wavelength, is found at 281.9 nm ( $n-\pi^*$ ), but in the calculations, it is at about 292.6 nm ( $\pi-\pi^*$ ) for B3LYP/6–31G\* level. Dependent upon the optimized structures, molecular orbital coefficient analyses point out that the electronic absorption spectra aforementioned are mainly assigned to the  $n-\pi^*$  and  $\pi-\pi^*$  electron transitions. Some frontier molecular orbital surfaces of the title compound obtained at the B3LYP/6–31G\* method are shown in Fig. 7, from which we can see that the electronic transitions mainly take place among the groups, which are corresponding to the intermolecular  $n-\pi^*$  and  $\pi-\pi^*$  electron transitions.

### 3.8. Thermodynamic properties

On the basis of statistically thermodynamic and vibrational analysis at the B3LYP/6–31G\* level, the standard thermodynamic functions of heat capacity ( $C_{p,m}^0$ ), entropy ( $S_m^0$ ) and enthalpy ( $H_m^0$ ) were obtained and listed in Table 6. The scale factor for the frequencies is 0.9613. As observed from Table 6, all the values of  $C_{p,m}^0$ ,  $S_m^0$ , and  $H_m^0$  increase when increasing the temperature from 100.0 to 500.0 K, which is attributed to the enhancement of molecular vibration as the temperature increases.



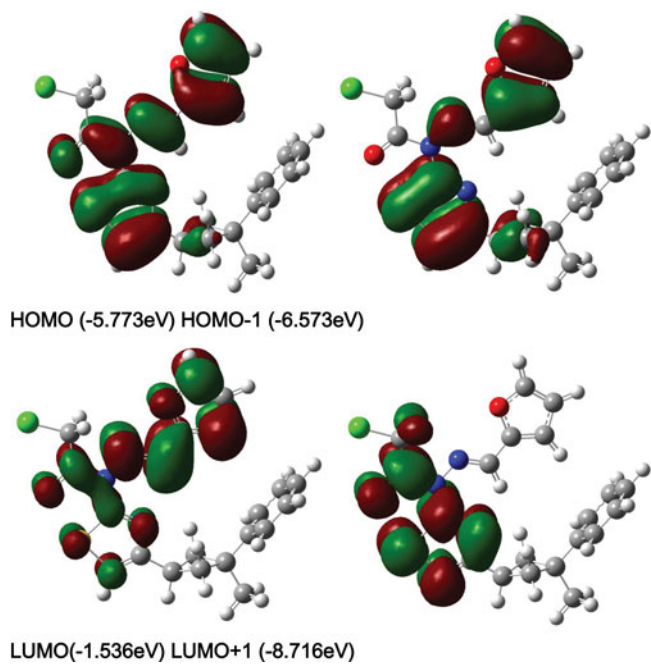


**Figure 7.** Molecular orbital surfaces and energy levels given in parentheses for the HOMO–1, HOMO, LUMO and LUMO+1 of the title compound computed at B3LYP/6–31G(d) level. The positive phase is red, and the negative phase is green.

The correlation linear equations between these thermodynamic properties and temperatures  $T$  are as below:

$$C_{p,m}^0 = 44.9694 - 0.0271T + 4.68836 \times 10^{-4}T^2 \quad (R = 0,91799)$$

$$S_m^0 = 135,1078 - 0,21735T - 8,5755 \times 10^{-4}T^2 \quad (R = 0,8015)$$

$$H_m^0 = 7,86456 - 0,06335T + 2,63064 \times 10^{-4}T^2 \quad (R = 0,96012)$$

These equations could be used for further studies on the title compound. For example, when the title compound will be used as a reactant to take part in a new reaction, these standard thermodynamic functions can be applied as referenced thermodynamic values to calculate the changes of entropies ( $\Delta S_T$ ), enthalpies ( $\Delta H_T$ ), and Gibbs free energies ( $\Delta G_T$ ) of the reaction.

**Table 6.** Thermodynamic properties of the title compound at different temperatures at the B3LYP/6–31G(d) level

$T$ (K)	$C_{p,m}^0$ (cal.mol <sup>-1</sup> .K <sup>-1</sup> )	$S_m^0$ (cal.mol <sup>-1</sup> .K <sup>-1</sup> )	$\Delta H_m^0$ (kcal.mol <sup>-1</sup> –
100.00	41.403	110.936	2.7566
200.00	69.766	149.587	8.4946
300.00	77.910	142.210	12.6249
400.00	99.177	168.222	21.7181
500.00	153.797	250.207	43.3891

## 4. Conclusions

The title compound, *N'*-furan-2ylmethylene-*N*-[4-(3-methyl-3-phenyl-cyclobutyl)-thiazol-2-yl]-chloro-acetic acid hydrazide, has been synthesized and characterized. X-ray single-crystal structure has been also obtained. DFT/B3LYP and HF calculations at the 6–31G(d) and 6–31G(d,p) levels show that the optimized geometries can closely resemble the molecular structure. Computed and experimental geometric parameters, vibrational frequencies,  $^1\text{H}$  NMR and  $^{13}\text{C}$  chemical shift values of the title compound were compared in order to test the different theoretical approaches (HF, DFT/B3LYP) reported here. More commonly, however, the IR and NMR spectra are used in conjunction with other forms of spectroscopy and chemical analysis to determine the structures of complicated molecules. The geometry of the solid state structure is subject to intermolecular forces, such as van der Waals interactions and crystal packing forces. Molecular orbital coefficient analysis suggests that the electronic spectra are assigned to the  $\pi \rightarrow \pi^*$  and  $n \rightarrow \pi^*$  electronic transitions. The calculated MEP map agrees well with the solid-state interactions. Thermodynamic properties at different temperatures have been calculated and the correlations between these thermodynamic properties and temperatures *T* are also obtained.

## Acknowledgment

This study was supported financially by the Research Centre of Ondokuz Mayıs University (project No: F-461).

## References

- [1] Wheate, N. J., Walker, S., Craig, G. E., & Oun, R. (2010). *Dalton Trans.*, 39, 8113.
- [2] <http://en.wikipedia.org/wiki/Cyclobutane>.
- [3] Young, D. C. et al. (2001). *Computational Chemistry: A Practical Guide for Applying Techniques to Real World Problems*, John Wiley & Sons Inc., New York.
- [4] Chis, V. et al. (2005). *J. Mol. Struct.*, 363, 744.
- [5] Sheldrick, G. M. (2008). *Acta Crys.*, A64, 112.
- [6] Wilson, A. et al. (1992). *J. International Table for X-ray Crystallography*; Kluwer Academic: Dordrecht, The Netherlands; Vol. C: Tables 6.1.1.4 (pp. 500) and 4.2.6.8 (pp. 219), respectively.
- [7] Jamorski, C., Casida, M. E., & Salahub, D. R. (1996). *J. Phys. Chem.*, 104, 5134.
- [8] Bauerschmitt, R., Häser, M., Treutler, O., & Alrichs, R. (1997). *Chem. Phys. Lett.*, 264, 573.
- [9] Becke, A.D. (1993). *J. Phys. Chem.*, 98, 5648.
- [10] Lee, C., Yang, W., & Parr, R. G. (1998). *Phys. Rev. B*, 37, 785.
- [11] Ditchfield, R. (1972). *J. Chem. Phys.*, 56, 5688.
- [12] Wolinski, K., Hinton, J. F., & Pulay, P. (1990). *J. Am. Chem. Soc.*, 112, 8251.
- [13] Dennington I. I. R., Keith T., & Millam, J. (2007). *GaussView, Version 4.1.2*, Semichem, Inc.: Shawnee Mission, KS.
- [14] Frisch, M. J. et al. (2004). *Gaussian 03 (Revision E.01)*. Gaussian, Inc., Wallingford, CT.
- [15] Cancs, E., Mennucci, B., & Tomasi, J. (1997). *J. Chem. Phys.*, 107, 3032.
- [16] Özdemir, N., Dinçer, M., & Cukurovali, A. (2010). *J. Mol. Model.*, 16, 291.
- [17] Demir, S., Dinçer, M., Cukurovali, A., & Yilmaz, I. (2006). *Acta Crystallogr.*, E62, o298.
- [18] Cukurovali, A., Özdemir, N., Yilmaz, I., & Dinçer, M. (2005). *Acta Crystallogr.*, E61, o1754.
- [19] Bernstein, J., Davis, R.E., Shimoni, L., & Chang, N.L. (1995). *Ang. Chem. Int. Ed. Eng.*, 34, 1555.
- [20] Spek, A.L. (2003). *J. Appl. Cryst.*, 36, 7.
- [21] Rovnyak, G. C. et al. (1995). *J. Med. Chem.*, 38, 119.
- [22] Kappe, C.O. (2000). *Eur. J. Med. Chem.*, 35, 1043.
- [23] Adams, S. et al. (2005). *J. Transl. Med.*, 3, 11, doi:10.1186/1479-5876-3-11.
- [24] Winter, C. A., Risley, E. A., & Nuss, G. W. (1962). *Proc. Soc. Exp. Biol. Med.*, 111, 544.

- [25] Jotani, Mukesh M., Baldaniya, Bharat B., Jasinski, & Jerry P. (2009). *J. Chem. Crystallogr.*, 39, 898.
- [26] Zhou, W. et al. (2004). *Vibr. Spectrosc.*, 34, 199.
- [27] Frisch, A., Nielsen, A. B., & Holder, A. J. (2001). *Gaussview User Manual*, Gaussian Inc.: Pittsburg.
- [28] de Dios, A. C. (1996). *J. Prog. Nucl. Magn. Reson. Spectrosc.*, 29, 229.
- [29] Helgaker, T., Jaszunski, & M., Ruud, K. (1999). *Chem. Rev.*, 99, 293.
- [30] Wolinski, K., Hinton, J. F., & Pulay, P. (1990). *J. Am. Chem. Soc.*, 112, 8251.
- [31] Barone, G. et al. G. (2002). *Chem. Eur. J.*, 8, 3233.
- [32] Barone, G. et al. (2002). *Chem. Eur. J.*, 8, 3240.
- [33] Taehtinen, P., Bagno, A., Klika, K. D., & Pihlaja, K. (2003). *J. Am. Chem. Soc.*, 125, 4609.
- [34] Cloran, F., Carmichael, I., & Serianni, A. S. (2001). *J. Am. Chem. Soc.*, 123, 4781.
- [35] Bagno, A. (2001). *Chem. Eur. J.*, 7, 1652.
- [36] Cimino, P., Gomez-Paloma, L., Duca, D., Riccio, R., & Bifulco, G. (2004). *Magn. Reson. Chem.*, 42, 26.
- [37] Hohenberg, P., & Kohn, W. (1964). *Phys. Rev.* 136, B864.
- [38] Becke, A. D. (1993). *J. Chem. Phys.*, 98, 5648.
- [39] Hehre, W. J. (1995). *Practical Strategies for Electronic Structure Calculation*. Wavefunction, Inc., Irvine, 102–134.
- [40] Dewar, M. J. S., Zoebisch, E. G., Healy, E. F., & Stewart, J. J. (1985). *J. Am. Chem. Soc.*, 107, 3902.
- [41] Nunes, Sandra C. C., Lopes Jesus, A. J., Rosado, Mário Túlio, S., Ermelinda, M., & Eusébio, S. (2007). *J. Mol. Structr.*, 806, 231.
- [42] Sarai, A. (1989). *J. Theor. Biol.*, 140, 137.
- [43] North, A. C. T. (1989). *J. Mol. Graph.*, 7, 67.
- [44] Kurtaran, R., Odabaşoğlu, S., & Azizoğlu, A. (2007). *Polyhedron*, 26, 5069.